Electronic Supplementary Material (ESI) for ChemComm.
This journal is © The Royal Society of Chemistry 2022

Supporting Information

Phenyl S-Te Bond with Unique Redox Activity in Dilute Electrolyte of Lithium Battery

*Qianhan Chen,[†] Yubing Si,[†] Wei Guo, and Yongzhu Fu**

Experimental section

Materials. Phenyl disulfide (PhS-SPh, $C_6H_5SSC_6H_5$, 99%, Sigma Aldrich), and phenyl ditelluride (PhTe-TePh, $C_6H_5TeTeC_6H_5$, 97%, Acros Organics) were purchased and used as received. The composition of electrolyte is 0.11 M lithium bis(trifluoromethanesulfonimide) (LiTFSI, $LiN(CF_3SO_2)_2$, 99%, Acros Organics) and 0.055 M lithium nitrate ($LiNO_3$, 99.999%, Acros Organics) in 1,2-dimethoxyethane (DME, 99.5%, Sigma Aldrich) and 1,3-dioxolane (DOL, 99.8%, Sigma Aldrich) (DME/DOL = 1:1 v/v). (Unless otherwise specified, the electrolyte was always used in this study.)

Li cell fabrication and electrochemical measurements. The bucky paper (NanoTechLabs, Inc) was punched into 1.13 cm^2 (d = 12 mm, mass = 2 mg.), then dried in a vacuum oven for 24 h at 100°C before use. Except for the high load test, the concentration of catholyte used in the battery tests is 0.5 M (mass of active material in 20 μL 0.5 M catholyte: PhS-SPh: 2.2 mg; PhTe-TePh: 4.1 mg; PhS-TePh: 3.1 mg). CR2032 coin cells were assembled in an Ar-filled glove box (H_2O<0.1 ppm, O_2<0.1 ppm). Firstly, the bucky paper was placed in the center of the positive case, 20 μL catholyte was added to the bucky paper and then Celgard 2400 as a separator was placed on top of the cathode. Then another 20 μL blank electrolyte was added on the separator. Finally, a lithium metal anode was placed on separator. The cells were encapsulated and taken out of the glove box and tested by LANHE battery cycler between 1.7 and 2.8 V at different current density. (Theoretical specific capacity: 245.5 mAh g^{-1} for PhS-SPh, 130.9 mAh g^{-1} for PhTe-TePh, and 170.7 mAh g^{-1} for PhS-TePh.) For the cyclic voltammetry (CV), the cell was swept from open circuit voltage (OCV) to 1.7 V and then back to 2.8 V at 0.1 mV s^{-1}.

Characterizations. The preparation process of phenyl tellurosulfide (PhS-TePh) is as follows: equimolar PhS-SPh and PhTe-TePh were mixed in DME solvent, and the solution was stirred for 4 h in an Ar-filled glove box. Then, DME was removed by drying overnight in the transition compartment of the glove box. The product was obtained for further characterization and analysis. Catholytes were prepared by dissolving appropriate amount of active material in the electrolyte.

The X-ray diffraction (XRD) data were collected by Rigaku SmartLabSE X-ray diffractometer with Cu Kα radiation source. The scanning rate was 2° min^{-1}, and 2θ was set between 10° and 60°. Nuclear magnetic resonance (NMR) spectra were collected on a Bruker Ascend TM 600 MHz. About 10 mg of raw material was dissolved into 600 μL $CDCl_3$ for NMR testing. The chemical shifts (δ) in NMR spectra were referenced to tetramethylsilane (TMS, $(CH_3)_4Si$) in deuterated reagents as an internal standard. X-ray photoelectron spectroscopy (XPS) measurements were conducted with AXIS SUPRA+.

Ultraviolet and visible spectrophotometry (UV-vis) was performed by Agilent 8453 spectrometer with a range between 200 cm^{-1} to 800 cm^{-1}. The mixture DOL/DME (1:1 v/v) solvent was used for baseline correction. The three materials were dissolved in the above-mentioned solvents to form 3 mM solution for the UV-vis testing. The raw materials were examined by the HORIBA HR Evolution within the range of 100–600 cm^{-1} with a 532 nm laser at 5% ND filter. For *in situ* Raman testing, the cell was assembled in an Ar-filled glove box using a specific *in situ* Raman mold. Therefore, the cell was always maintained under the same working environment as the coin cell during the test.

Quadrupole time-of-flight mass spectrometry (QTof-MS, Waters Xevo G2-XS QTof mass spectrometer) was used to analyze the cycled samples. The cells cycled at 0.1 mA cm^{-1} for 1 cycle and were disassembled in the glove box. The charged and discharged electrodes were immersed in 100 μL chromatographic methanol to dissolve the active material. The solution was dipped with a solid sampling rod and loaded into the instrument directly. The ion source of ASAP was used for testing. The same method was used for other samples in the MS measurements.

Theoretical simulations. To gain insight into the effects of the electronic structure, the density functional theory (DFT) calculations was performed. DFT calculations using hybrid

functionals of M062X at the def2-SVP level was employed to optimize the ground state by Gaussian 16 program,[1] the solvent effect was mimicked with the solvation model based on density (SMD) with ε = 7.07.[2, 3] The electrostatic potential (ESP) and electron localization function (ELF) as well as Mayer bond order analyses were performed by Multiwfn program, and the 3D-presentation of the molecular orbitals were generated by GaussView 5.0 program.[4, 5]

To better understand the effect of concentration on the battery performance, ab initio molecular dynamic (AIMD) simulations were performed with the CP2K package.[6] Two boxes with 40Å × 40Å × 40Å were created, with the high-concentration system consisting of 144 DOL molecules, 96 DME molecules, 20 LiTFSI, 1 $LiNO_3$, and 10 PhS-TePh to mimic the 1.1 M lithium salt environment. And the low-concentration system consists of 129 DOL molecules, 87 DME molecules, 2 LiTFSI, 1 $LiNO_3$, and 9 PhS-TePh molecules to mimic the 0.16 M lithium salt environment. The initial complexes for the AIMD simulations were pre-equilibrated by extended semiempirical tight-binding molecular dynamic simulations within periodic boundary conditions, using the GFN1-xTB model of the CP2K program package. After 600 ps in NPT ensemble (1 atm, 298.15 K), the final snapshot of the trajectories was selected as an initial geometry for AIMD simulations. The simulations temperature was set to 298.15 K, and a time step of 1 fs was chosen. The system was then simulated for 200 ps at 298.15 K in an NVT ensemble by using Nosé–Hoover thermostats. The forces were computed via the QuickStep module,[7] the valence electrons were considered explicitly, and the core electron states were represented via Goedecker-Teter-Hutter pseudopotentials.[8] The Grimme dispersion correction was used in conjunction with the molecularly optimized double-ζ basis set (MOLOPT-DZVP-SR-GTH) was applied to all atoms together with the revised Perdew, Burke, and Ernzerhof (revPBE) functional. The initio box was created by Packmol program and the input file for CP2K simulation was built by Multiwfn as well as the data analyses was performed with VMD program.[9]

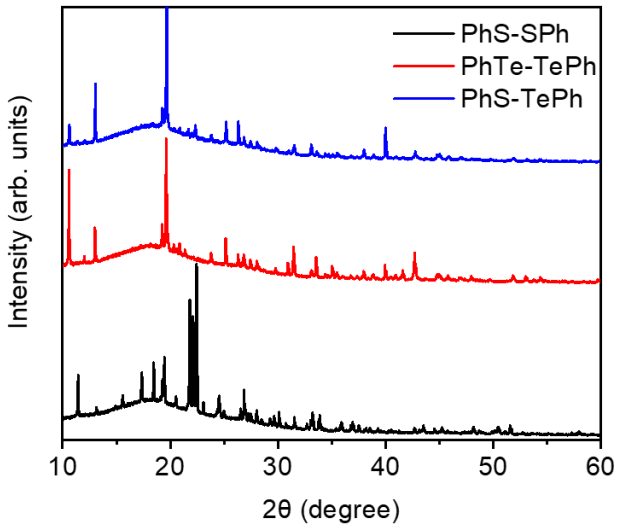

Figure S1. X-ray diffraction patterns of PhS-SPh, PhTe-TePh, and PhS-TePh.

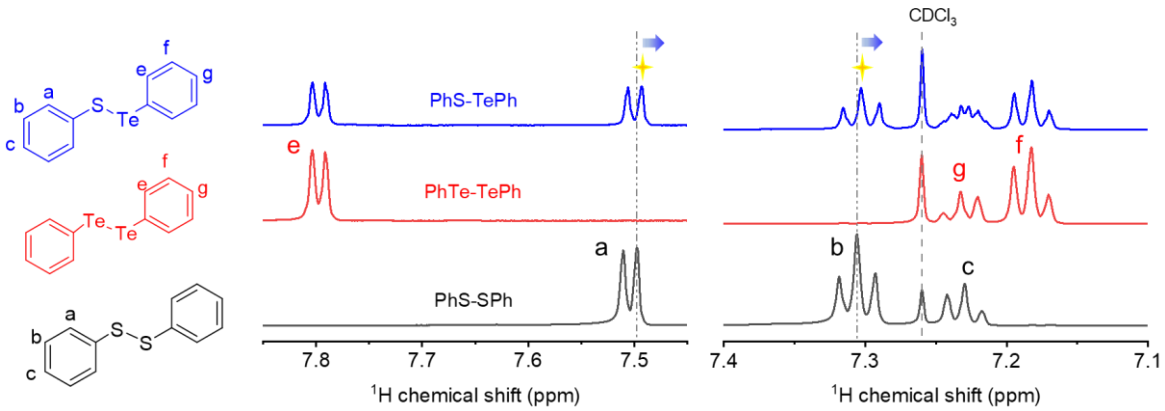

Figure S2. ^{1}H NMR spectra of PhS-SPh, PhTe-TePh, and PhS-TePh.

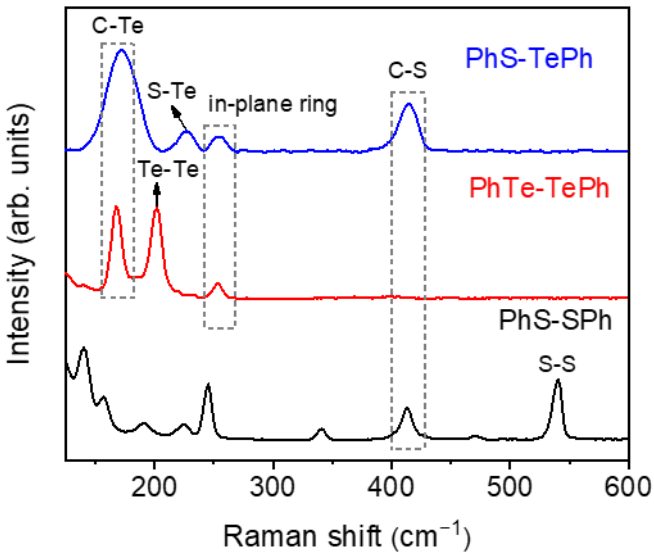

Figure S3. Raman spectra of PhS-SPh, PhTe-TePh, and PhS-TePh.

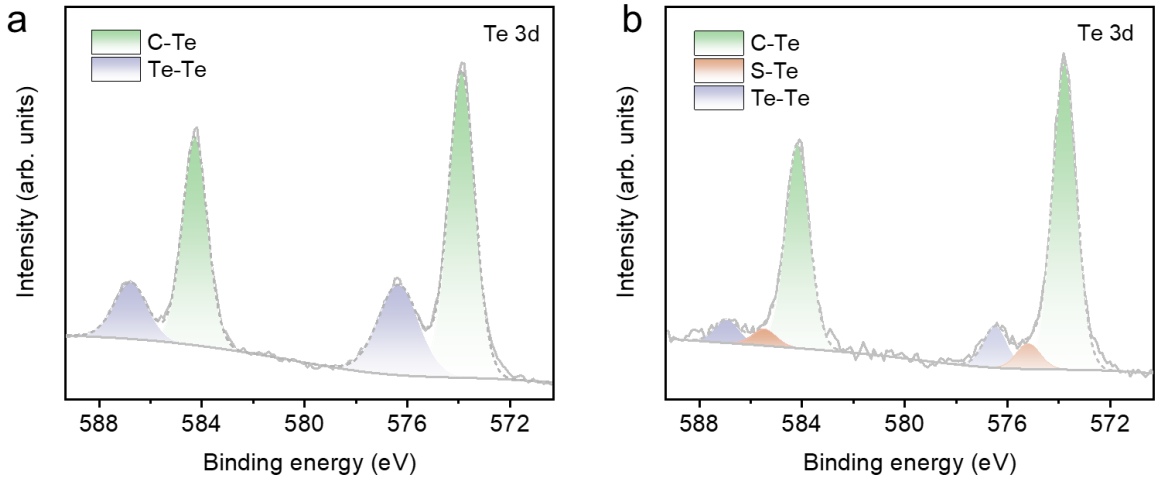

Figure S4. X-ray photoelectron spectroscopy (XPS) spectra of Te 3d of (a) PhTe-TePh and (b) PhS-TePh.

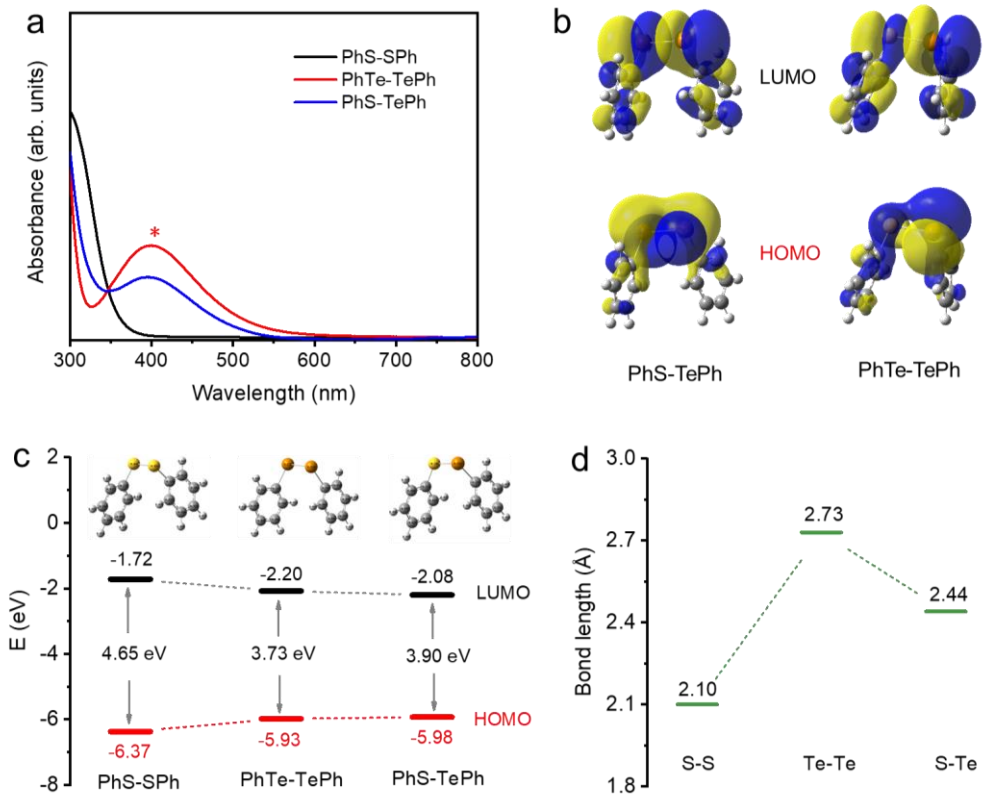

Figure S5 (a) UV–vis absorption spectra of 2 mM PhS-SPh, PhTe-TePh, and PhS-TePh. (b) The 3D electron density map of the LUMO and HOMO of PhS-TePh and PhTe-TePh (isovalue = 0.02). (c) LUMO and HOMO energy levels. (d) Bond lengths of S-S, Te-Te, and S-Te bonds for the optimized local minima.

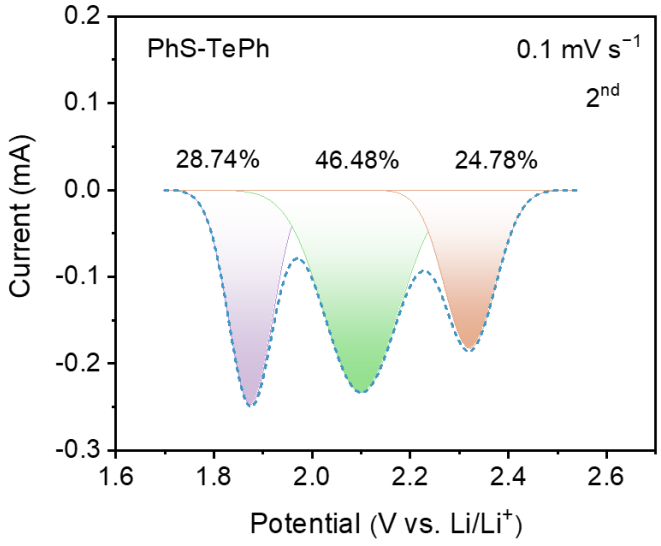

Figure S6. Fitted integral plot of reduction peaks in the CV of the Li/PhS-TePh cell.

Table S1. The parameter ratios corresponding to the fitting integral plot of the reduction peaks of the Li/PhS-TePh cell.

Peak	Voltage range	Peak area	Peak area percentage	Corresponding transfer electron ratio
1	1.70–1.96 V	0.02756	28.74141%	1
2	1.96–2.44 V	0.04457	46.48361%	2
3	2.44–2.53 V	0.02376	24.77497%	1

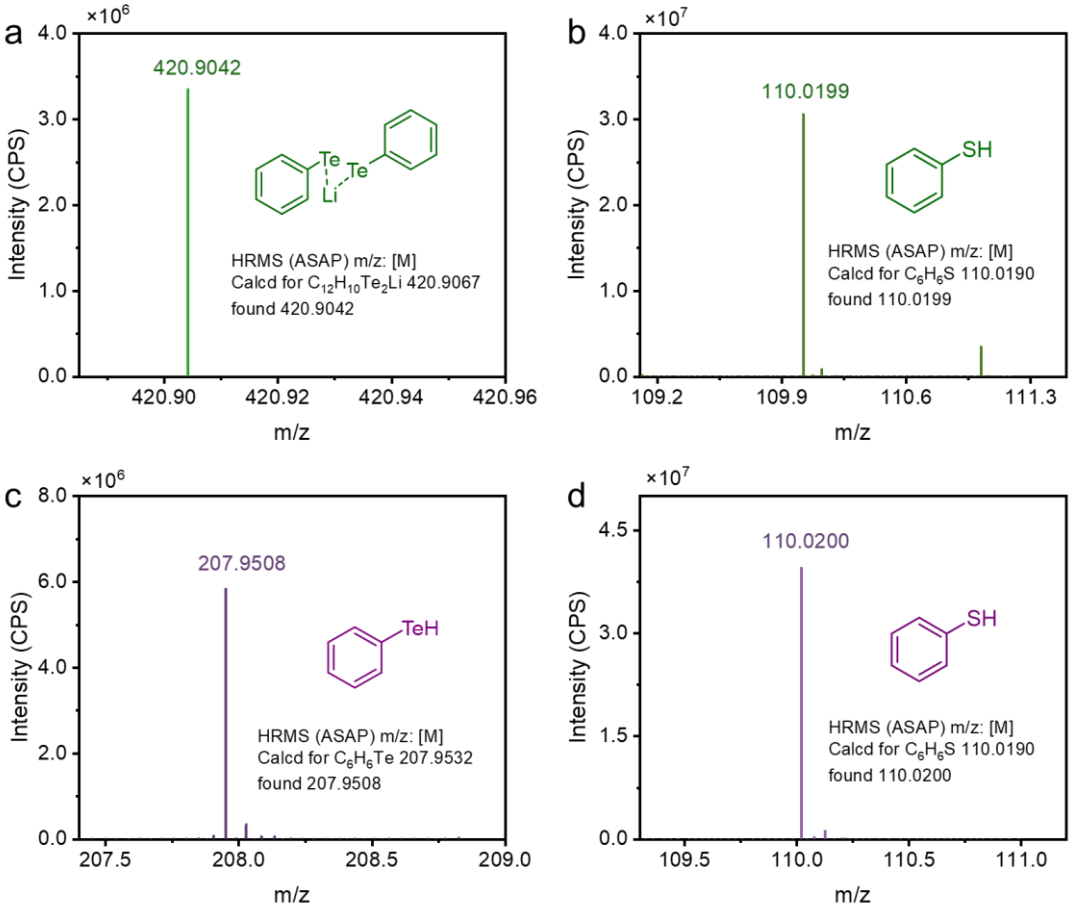

Figure S7. MS spectra of the discharge products of the Li/PhS-TePh cell. (a, b), (c, d) correspond to the discharge products of the second and third discharge plateaus, respectively.

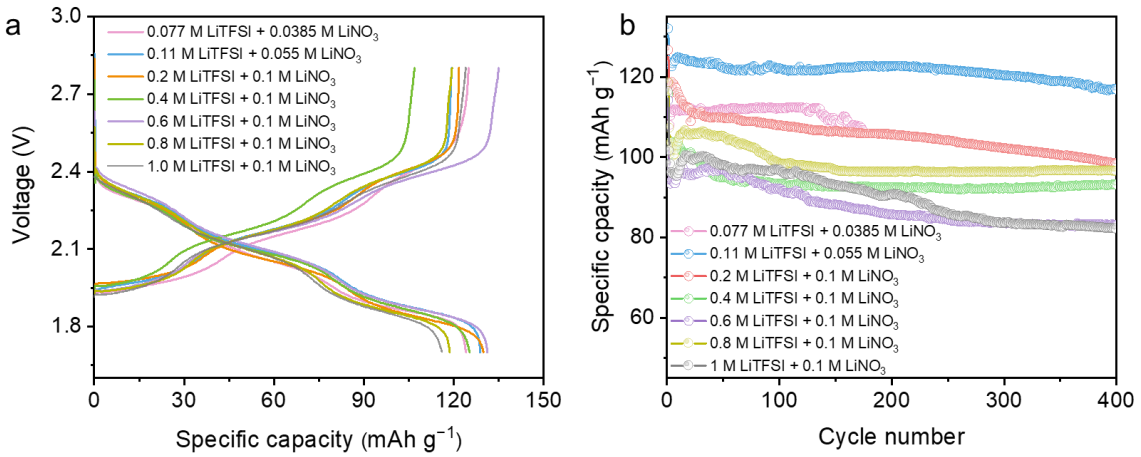

Figure S8. (a) Voltage profiles and (b) cycling performance of the cell with 0.5 M PhS-TePh with different concentrations of electrolyte in lithium cells at 0.1 mA cm^{-2}.

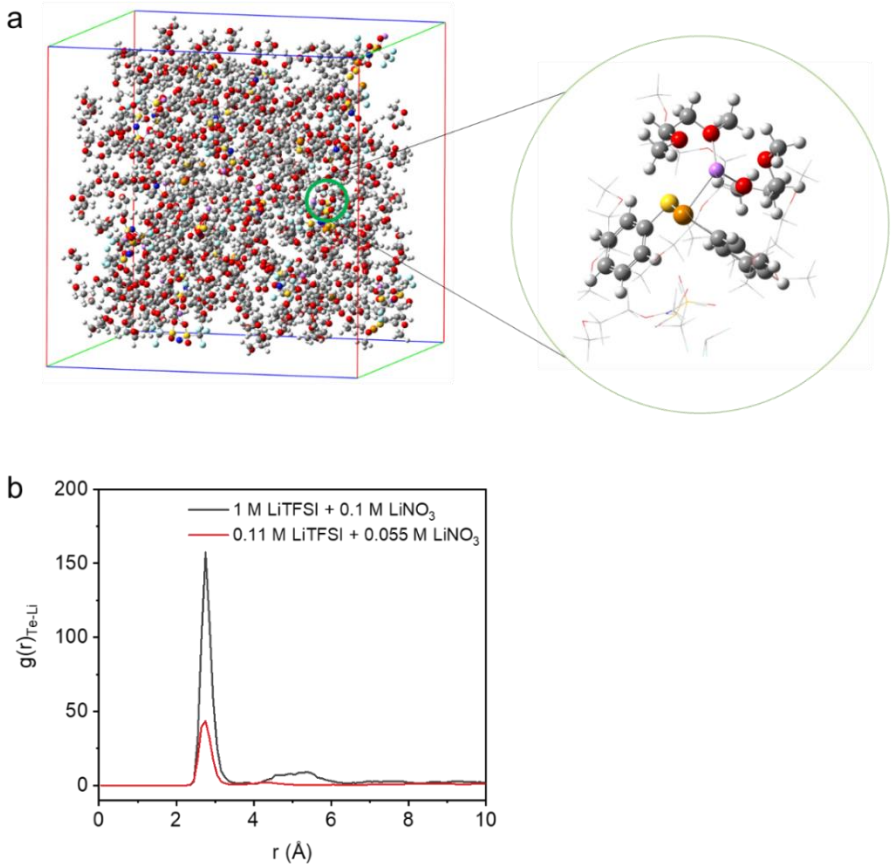

Figure S9. (a) The snapshot of MD simulations for PhS-TePh@high concentration electrolyte (1 M LiTFSI, 0.1 M $LiNO_3$ in DOL/DME=1:1 vol%). Color codes for atoms: gray, C; purple, Li; orange, Te; yellow, S; red, O; white, H. (b) Radial distribution functions calculated from MD simulations for different concentrations of lithium salts.

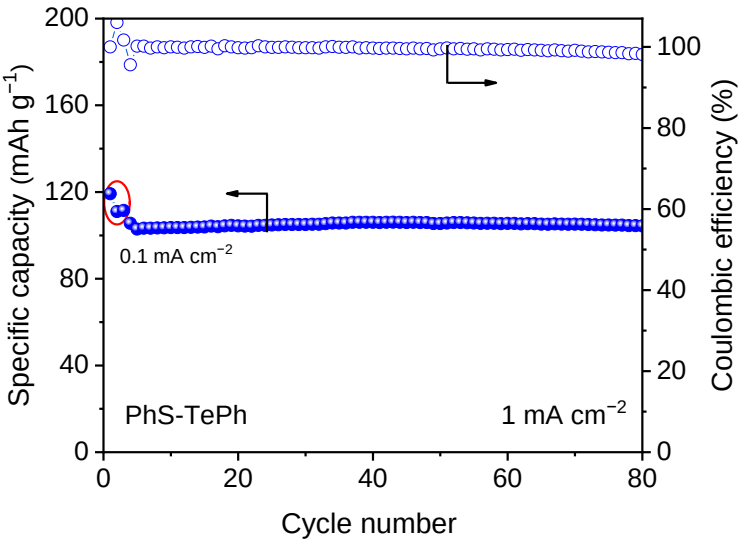

Figure S10. Cycling performance of the cell with 0.5 M PhS-TePh at 1 mA cm^{-2}.

References

1. R. Dennington, T. A. Keith, J. M. Millam and S. Inc, *GaussView, Version 5.0.*, Shawnee Mission, KS, 2016.
2. Y. Cui, J. D. Ackerson, Y. Ma, A. Bhargav, J. A. Karty, W. Guo, L. Zhu and Y. Fu, *Adv. Funct. Mater.*, 2018, **28**, 1801791.
3. A. V. Marenich, C. J. Cramer and D. G. Truhlar, *J. Phys. Chem. B*, 2009, **113**, 6378-6396.
4. T. Lu and F. Chen, *J. Comput. Chem.*, 2012, **33**, 580-592.
5. M. J. Frisch, G. W. Trucks, H. B. Schlegel, G. E. Scuseria, M. A. Robb, J. R. Cheeseman, G. Scalmani, V. Barone, G. A. Petersson and H. Nakatsuji, *Gaussian 16 Rev.*, A.03, Wallingford, CT, 2016.
6. T. D. Kuhne, M. Iannuzzi, M. Del Ben, V. V. Rybkin, P. Seewald, F. Stein, T. Laino, R. Z. Khaliullin, O. Schutt and F. Schiffmann, *J. Chem. Phys.*, 2020, **152**, 194103.
7. J. VandeVondele, M. Krack, F. Mohamed, M. Parrinello, T. Chassaing and J. Hutter, *Comput. Phys. Commun.*, 2005, **167**, 103-128.
8. B. G. Lippert, J. H. Parrinello and Michele, *Mol. Phys.*, 2010, **92**, 477-488.
9. W. Humphrey, A. Dalke and K. Schulten, *J. Mol. Graph.*, 1996, **14**, 33-38.